

this symmetry is in fact present.

Acknowledgment. We thank the National Institutes of Health for financial support of this work under Grant GM 29541, and the Humboldt Foundation for a Lynen grant to J.J.W. NSF Major Equipment grants were used for purchase of the computational and spectral equipment. We are indebted to Dr. H. Reis (BASF, Ludwigshaven) for providing the cyclooctatetraene used in this work, to Professor W. Grimme (Universität Köln) for providing unpublished basketene preparations (ref 3c,d), and to

Dr. T. Clark (Universität Erlangen-Nürnberg) for modifying VAMP for the Stardent computer, for supplying us his program, and for fruitful discussions on its proper use.

Supplementary Material Available: X-ray crystallographic structural data (numbered thermal ellipsoid plot, atomic coordinates, bond lengths, bond angles, anisotropic displacement coefficients) for **9a** and **9s** (8 pages). Ordering information is given on any current masthead page.

¹H NMR Hyperfine Shift Pattern as a Probe for Ligation State in High-Spin Ferric Hemoproteins: Water Binding in Metmyoglobin Mutants

Krishnakumar Rajarathnam,[†] Gerd N. La Mar,^{*†} Mark L. Chiu,[‡] Stephen G. Sligar,[‡] Jai P. Singh,[†] and Kevin M. Smith[†]

Contribution from the Department of Chemistry, University of California, Davis, California 95616, and the Departments of Chemistry, Biochemistry, Physiology, and Biophysics and The Beckman Institute for Advanced Science and Technology, University of Illinois, Urbana, Illinois 61801. Received April 10, 1991

Abstract: The ¹H NMR spectra of a series of high-spin ferric metmyoglobins (metMb_s) have been analyzed to assess the validity of meso proton (meso-H) contact shift direction as a probe for H₂O coordination and to develop a quantitative interpretative basis of the hyperfine shift pattern as a structural probe for the heme-iron ligation state. The quantitative analyses of the hyperfine shifts are based on a comparison of the structurally characterized six-coordinate sperm whale metMbH₂O and the five-coordinate *Aplysia* metMb. The developed spectral probes are subsequently applied to elucidate the role of distal residues in modulating H₂O coordination in a series of E7 and E11 point mutants of sperm whale Mb. The elusive distal E11 residue signals are assigned in the two reference proteins on the basis of their unique relaxation properties and from the spectral characteristics of E11 sperm whale Mb point mutants. Quantitative analysis of the E11 residue dipolar shifts demonstrates that the loss of coordinated H₂O leads to a substantial increase in the zero-field splitting constant, *D*. The change from strongly low-field meso-H shifts in six-coordinate sperm whale metMbH₂O to strongly upfield meso-H shifts in five-coordinate *Aplysia* metMb is accompanied by predicted changes in chemical shifts for heme methyl, F8 His C_βH, and E11 Val methyl protons. The most readily recognized change is the 5-ppm low-field bias of the mean methyl shift upon loss of water coordination. The consistency in the changes of all the NMR spectral parameters supports the use of the meso-H chemical shifts as probes for ligation state but suggests that all accompanying changes should be analyzed. Substitution of E11 Val by Ile, Phe, or Ala results in minimal perturbation with full retention of coordinated water. Substitution of E7 His by Val or Phe abolishes H₂O coordination, while replacement by Gln or Gly leads to a fractional H₂O coordination. The sensitivity of the hyperfine shifts of the heme methyl protons to solvent isotope composition supports the proposed changes in H₂O ligation. The application of the heme mean methyl shifts as a probe for H₂O coordination in a series of natural genetic variants differing in E7 residue confirms previous conclusions, except for elephant metMb (E7 Gln) which is concluded here to be primarily five-coordinate rather than six-coordinate. The occupation of the sixth position by water as a function of E7 residue is found to be very similar in sperm whale E7 point mutants and natural genetic variants, and it is concluded that H bonding by E7 residue is the strongest but not the only stabilizing influence on H₂O coordination.

Introduction

Myoglobin (Mb) is a small hemoprotein whose primary function is to store molecular O₂ in skeletal muscle in its functional ferrous form.¹ This protein, in both the reduced and oxidized states, binds many other small neutral ligands and anions, and much of our understanding of the relationship between structure and function in the O₂ binding hemoproteins has been derived from the studies of these nonphysiological ligands.² One potential ligand which has considerable functional significance, albeit indirectly, is the H₂O molecule. While it does not directly compete with O₂ for the reduced heme-Fe binding site, H₂O is H bonded to the distal residue in a manner that requires its displacement by the ligand before it can bind to the Fe. However, this type of interaction is highly selective in that a H₂O molecule is found H bonded to the distal His E7³ in the α subunit but not the β subunit of human

deoxy hemoglobin (Hb);⁴ sperm whale (SW) deoxy Mb exhibits fractional occupancy of such a site.⁵ It is clear that access of H₂O to the heme cavity influences the dynamics and thermodynamics of ligation. The access of H₂O to the distal cavity, and associated dissolved anions, has also been implicated in the autoxidation of Mb and Hb,⁶ where the ferrous heme is oxidized

(1) Kagen, L. J. *Myoglobin: Biochemical, Physiological, and Clinical Aspects*; Columbia University Press: New York, 1973.

(2) Antonini, E.; Brunori, M. *Hemoglobin and Myoglobin in Their Reactions with Ligands*; North Holland Publishing Company: Amsterdam, 1971.

(3) E7, E11, and F8 are the alphanumeric codes referring to the position of the residues in the sperm whale myoglobin amino acid sequence. E7 is the seventh residue in the E helix, F8 is the eighth residue in the F helix, and so on (Edmundson, A.E. *Nature* **1965**, *205*, 883).

(4) Fermi, G.; Perutz, M. F.; Shannan, B.; Fourme, R. *J. Mol. Biol.* **1984**, *175*, 159-174.

(5) Takano, T. *J. Mol. Biol.* **1977**, *110*, 569-584.

[†]University of California.

[‡]University of Illinois.

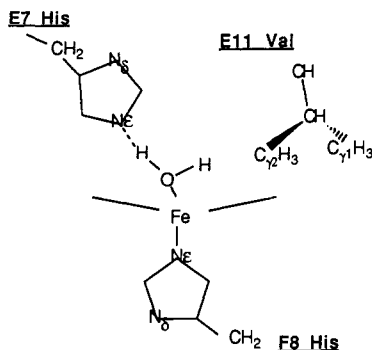


Figure 1. Schematic representation of the distal cavity and the proposed H bonding (shown by dotted lines) between the iron(III)-bound H_2O and the N_ϵ of the distal histidine.

to the ferric form, giving rise to metMb and metHb.

A more direct role for H_2O is found in the oxidized metMb and metHb, where it is often found coordinated to the iron(III) at low pH to yield the met-aquo species. The bound H_2O molecule has been identified in the X-ray crystal structure of both SW⁷ and horse metMb,⁸ and its stability in the bound form is rationalized by a H-bonding interaction with the conserved distal His E7, as shown in Figure 1. On the other hand, the crystal structure of the metMb from the sea hare, *Aplysia limacina*, has revealed a five-coordinated iron,⁹ and the absence of the coordinated H_2O is attributed to the unusual presence of distal E7 Val residue which renders the heme pocket hydrophobic and eliminates potential stabilization of the bound H_2O via H bonding. The lack of bound H_2O ¹⁰⁻¹² is also manifested in the kinetics of ligand binding to the iron(III) in ferric proteins as the on-rates of NO , N_3^- , and F^- are $\sim 10^2$ to 10^3 times higher in five-coordinate than those in six-coordinate proteins.

For metMbs and metHbs which lack crystal structures, the presence of a coordinated H_2O has been inferred from a number of spectroscopic techniques, including ^1H NMR,¹³⁻¹⁸ resonance Raman,^{19,20} and visible absorption^{10,21} spectroscopies. The pattern of ^1H NMR hyperfine shift of high-spin ferric hemoproteins provides a wealth of information on the active site electronic and molecular structure.²² Extensive studies of model heme complexes²³ have revealed an empirical indicator that discriminates between five- and six-coordinated ferric hemes, which was proposed

to serve as a probe for H_2O coordination in metMbs and Hbs. This empirical probe involves the characteristic difference in the sign of the heme meso-H contact shifts, which are found ~ 30 to 40 ppm low-field in six-coordinated and ~ 20 to 70 ppm upfield in five-coordinated systems. Detailed assignments of heme resonances based on reconstitution with specifically deuterated hemes have shown that the meso-H shifts are indeed low-field (~ 40 ppm) in SW metMb H_2O ¹³ and upfield (~ -30 ppm) in *Aplysia*¹⁴ metMb for which the sixth site is vacant. Additional support for ^1H NMR identification of coordinated H_2O involves detection of substantial solvent isotope effects on the heme methyl chemical shifts.²⁴

There exists at present no satisfactory interpretive basis for the difference in meso-H chemical shift direction and heme coordination number. However, the direction of the meso-H shift has correlated with a H-bonding interaction in all structurally characterized systems. In this report we investigate in detail the ^1H NMR spectral parameters that accompany changes in the occupancy of the sixth ligation site in a pair of well-characterized high-spin ferric Mbs, the six-coordinate SW metMb H_2O and the five-coordinate *Aplysia* metMb, for which high-resolution X-ray crystal coordinates exist,^{5,9} and for which at least the heme resonances have been unambiguously assigned. A detailed analysis of electronic structure of SW metMb H_2O has so far been hampered by the inability to assign the hyperfine-shifted non-heme signals. Of particular interest are the noncoordinated distal amino acid residues for which the large zero-field splitting imparts substantial upfield dipolar shifts.²⁵ The recent successful over-expression in *E. coli* of SW Mb based on a synthetic gene²⁶ has permitted the construction of a variety of point mutants at the key distal positions, E7 and E11. These distal mutants provide for the first time the necessary variants that allow assignment of the key distal residue peaks in SW metMb H_2O and *Aplysia* metMb, besides serving as ideal examples for testing the correlation between distal environment and the ligation of H_2O at the sixth site.

Our interests in this report are 2-fold: to develop a more quantitative interpretive basis of the ^1H NMR spectral parameters that relate to the ligation state of the sixth position in high-spin ferric hemoproteins, and to explore the correlation between the nature of distal residues and the coordination of H_2O in metMb complexes for a variety of synthetic point mutants and natural genetic variants. The quantitative analysis of the hyperfine shifts, including the assignment of distal residue signals, is carried out for the five- and six-coordinated prototype heme complexes, *Aplysia* metMb and SW metMb H_2O , respectively, for which the necessary structural details are available. The assignment of distal residue signals is carried out by substitution at the E11 position in SW Mb, E11 Val \rightarrow Ala (Val[E11]Ala), \rightarrow Ile (Val[E11]Ile), and \rightarrow Phe (Val[E11]Phe), and the influence(s) of distal residue on H_2O coordination is studied in point mutants E7 His \rightarrow Val (His[E7]Val), \rightarrow Gly (His[E7]Gly), \rightarrow Gln (His[E7]Gln), and \rightarrow Phe (His[E7]Phe).

Experimental Section

SW Mb was purchased from Sigma Chemical Co. as a lyophilized powder and used without further purification. E7 and E11 mutants were obtained as reported earlier.²⁶ metMbs were prepared by oxidizing the protein with 3 equiv of potassium ferricyanide and exchanging in an Amicon ultrafiltration device at least six times with a 0.1 M potassium phosphate buffer in $^2\text{H}_2\text{O}$ at pH 6.2. The meso- $^2\text{H}_4$ -hemin was prepared by acid-catalyzed deuteration²⁷ of the corresponding 2,4-bis(2-chloroethyl)deuteroporphyrin-IX dimethyl ester followed by vinylation in base and iron insertion/hydrolysis.²⁸ Apomyoglobin was prepared essentially according to Teale²⁹ and reconstituted with the meso- $^2\text{H}_4$ -hemin following

(6) Wallace, W. J.; Houtchens, R. A.; Maxwell, J. C.; Caughey, W. S. *J. Biol. Chem.* **1982**, *257*, 4966-4977.

(7) Takano, T. *J. Mol. Biol.* **1977**, *110*, 537-568.

(8) Evans, S. V.; Brayer, G. D. *J. Mol. Biol.* **1990**, *213*, 885-897.

(9) Bolognesi, M.; Onesti, S.; Gatti, G.; Coda, A.; Ascenzi, P.; Brunori, M. *J. Mol. Biol.* **1989**, *205*, 529-544.

(10) Giacometti, G. M.; Ascenzi, P.; Brunori, M.; Rigatti, G.; Giacometti, G.; Bolognesi, M. *J. Mol. Biol.* **1981**, *151*, 315-319.

(11) Sharma, V. S.; Traylor, T. G.; Gardinoer, R.; Mizukami, H. *Biochemistry* **1987**, *26*, 3837-3843.

(12) Benko, B.; Maricic, S. *Croat. Chem. Acta* **1978**, *51*, 369-377.

(13) La Mar, G. N.; Budd, D. L.; Smith, K. M.; Langry, K. C. *J. Am. Chem. Soc.* **1980**, *102*, 1822-1827.

(14) Pande, U.; La Mar, G. N.; Lecomte, J. T. J.; Ascoli, F.; Brunori, M.; Smith, K. M.; Pandey, R. K.; Parish, D. W.; Thanabal, V. *Biochemistry* **1986**, *25*, 5638-5646.

(15) Yamamoto, Y.; Osawa, A.; Inoue, Y.; Chujo, R.; Suzuki, T. *Eur. J. Biochem.* **1990**, *192*, 225-229.

(16) Constantinidis, I.; Satterlee, J. D.; Pandey, R. K.; Leung, H. K.; Smith, K. M. *Biochemistry* **1988**, *27*, 3069-3076.

(17) Krishnamoorthi, R.; La Mar, G. N.; Mizukami, H.; Romero, A. *J. Biol. Chem.* **1984**, *259*, 265-270.

(18) Lecomte, J. T. J.; La Mar, G. N.; Smit, G. J.; Winterhalter, K. H.; Smith, K. M.; Langry, K. C.; Leung, H. K. *J. Mol. Biol.* **1987**, *197*, 101-110.

(19) Morikis, D.; Champion, P. M.; Springer, B. A.; Egeberg, K. D.; Sligar, S. G. *J. Biol. Chem.* **1990**, *265*, 12143-12145.

(20) Rousseau, D. L.; Ching, Y.-c.; Brunori, M.; Giacometti, G. M. *J. Biol. Chem.* **1989**, *264*, 7878-7881.

(21) Shikama, K.; Matsuoka, A. *J. Mol. Biol.* **1989**, *209*, 489-491.

(22) Satterlee, J. D. *Concepts Magn. Reson.* **1990**, *2*, 69-79.

(23) Budd, D. L.; La Mar, G. N.; Langry, K. C.; Smith, K. M.; Nayyar-Mazhir, R. *J. Am. Chem. Soc.* **1979**, *101*, 6091-6096.

(24) La Mar, G. N.; Chatfield, M. J.; Peyton, D. H.; de Ropp, J. S.; Smith, W. S.; Krishnamoorthi, R.; Satterlee, J. D.; Erman, J. E. *Biochim. Biophys. Acta* **1988**, *956*, 267-276.

(25) Ann Walker, F.; La Mar, G. N. *Ann. N.Y. Acad. Sci.* **1973**, *206*, 328-348.

(26) Springer, B. A.; Sligar, S. G. *Proc. Natl. Acad. Sci.* **1987**, *84*, 8961-8965.

(27) Singh, J. P.; Smith, K. M. Unpublished results.

(28) Smith, K. M.; Langry, K. C. *J. Chem. Soc. Perkin Trans. 1* **1983**, 439-444.

(29) Teale, F. W. J. *Biochim. Biophys. Acta* **1959**, *35*, 543.

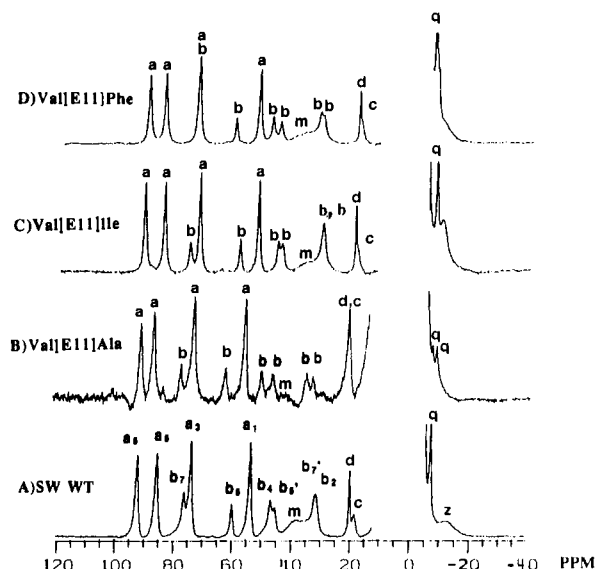


Figure 2. Hyperfine shifted region of the 360-MHz ^1H NMR spectra in $^2\text{H}_2\text{O}$ of the acidic form of wild type (WT) SW metMb and the E11 mutants at 25 $^\circ\text{C}$ in 0.1 M potassium phosphate buffer, pH 6.2: (A) SW metMbH $_2\text{O}$, (B) Val[E11]Ala metMb, (C) Val[E11]Ile metMb, (D) Val[E11]Phe metMb. Labeled are heme methyl (a), propionate and vinyl C $_2\text{H}$ (b), F8 His C $_\beta\text{H}$ (c), propionate C $_2\text{H}$ (d), meso-H (m), and distal E7 methyl protons (z); the subscript on the labels indicates the position, if known, of the corresponding proton on the heme. Note that all the chemical shifts of E11 mutants are very similar to the WT in the low-field region. In the upfield region, C $_2\text{H}_3$ methyl of E11 Val, z is labeled in the WT and note the absence of a corresponding peak in Val[E11]Ala and a narrower upfield peak in the Val[E11]Ile and Val[E11]Phe mutants.

established procedures¹⁸ and finally exchanged into a 0.1 M potassium phosphate buffer in $^2\text{H}_2\text{O}$ at pH 6.2. The pH values were measured with a Beckmann 3550 pH meter equipped with an Ingold 620 microcombination electrode and are uncorrected for any isotope effect.

^1H NMR spectra were recorded on a Nicolet NT-360 spectrometer operating at 360 MHz in quadrature mode. Data were collected by using double precision on 16384 points over a spectral window of 50 kHz. The NMR spectra were collected by using a modified version of the inversion-recovery pulse sequence, $90_x-240_y-90_x-\tau-90\text{-acq}$. The τ period corresponds to 30 ms and was found to be optimal in reducing the residual H $_2\text{O}$ signal without using a decoupler pulse. The spectra in Figure 4 were collected by using the standard inversion-recovery sequence, $180-\tau-90\text{-acq}$, where τ is the delay between the 180 and 90 pulses.

For the nuclear Overhauser (NOE) experiments,³⁰ spectra were collected by applying a decoupler presaturation pulse of 34 ms to the desired resonance and subtracting from the corresponding reference spectra with the decoupler pulse off-resonance. The signal-to-noise ratio was improved by apodizing all the free induction decays (FIDs) which introduces a 50-Hz line broadening; this is taken into account in the calculation of the reported line widths. Chemical shifts in all spectra are referenced to DSS (2,2-dimethyl-2-silapentane-5-sulfonate) through the residual solvent signal. The line widths and areas of the peaks were measured using the Nicolet NMCCAP curve-fitting program.

Results

Spectral Overview. The resolved portions of the ^1H NMR spectra of SW Mb mutants at positions E11 and E7 are illustrated in Figures 2 and 3, respectively. Included in each figure is the trace for six-coordinate WT SW metMbH $_2\text{O}$ (trace A), as well as the five-coordinate *Aplysia* metMb (trace B) in Figure 3. There is no evidence for heme disorder (rotation of the heme about the α - γ axis) in the spectra of the mutants, and if present it should be less than 5%. Previous studies^{13,14,23} have shown that the strong dominance of the contact interaction leads to relatively narrow low-field (four) methyl and (six) propionate and vinyl H $_a$ single proton heme resonances, for both five- and six-coordinate models, as well as in SW and *Aplysia* metMbs. Moreover, the C $_2\text{H}$ of

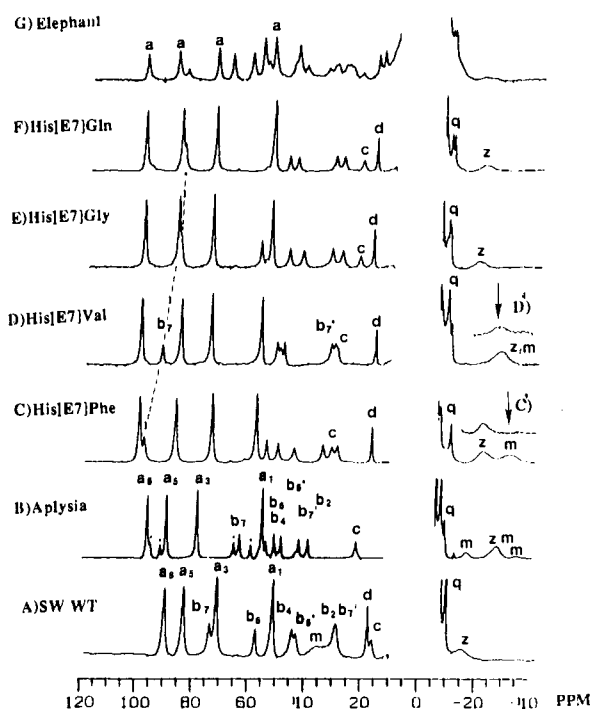


Figure 3. Hyperfine shifted region of the 360-MHz ^1H NMR spectra in $^2\text{H}_2\text{O}$ of the acidic form of WT SW metMb, *Aplysia* metMb, elephant metMb, and the E7 SW metMb mutants at 25 $^\circ\text{C}$ in 0.1 M potassium phosphate buffer, pH 6.2: (A) SW metMbH $_2\text{O}$, (B) *Aplysia* metMb, (C) His[E7]Phe metMb, (D) His[E7]Val metMb, (E) His[E7]Gly metMb, (F) His[E7]Gln metMb, and (G) elephant metMb. Labeled are heme methyl (a), propionate and vinyl C $_2\text{H}$ (b), F8 His C $_2\text{H}$ (c), propionate C $_2\text{H}$ (d), meso-H (m), and distal E7 methyl protons (z); the subscript on the labels indicates the position, if known, of the corresponding proton on the heme. Note that the methyl chemical shifts (a) of all the E7 mutants are more downfield shifted compared to the WT and are similar to those of *Aplysia* metMb, a known five-coordinate metMb. The dots in the spectrum of *Aplysia* indicate the methyl peaks from the minor component. The broad C $_2\text{H}_3$ methyl peak of E11 Val (z) is labeled in the WT SW, *Aplysia*, and the mutant Mbs. The meso peaks (m) are labeled and the inset (C' and D') shows the NMR spectra of His[E7]Phe and His[E7]Val mutants when reconstituted with meso- $^2\text{H}_4$ hemin. The complete disappearance of the most upfield shifted broad peak (\sim -30 ppm) in His[E7]Phe and a reduction in intensity of the peak z in His[E7]Val (indicated by an arrow) identify them as the meso-H's (m). The chemical shifts of 7-C $_2\text{H}$ propionate in the mutants are connected by a dotted line.

the proximal His (F8) is also found with similar line widths in the low-field region. All the mutants exhibit these four low-field methyl peaks (a) and seven single-proton resonances (six H $_a$ (b), one His F8 C $_2\text{H}$ (c)). Moreover, the unique orientation of the 7-propionate in SW metMbH $_2\text{O}$ results in one resolved propionate H $_2$ resonance (d), which is much narrower than resonances a, b, and c. Resonances such as d are observed for all mutant Mbs. The remaining low-field signals observed in SW metMbH $_2\text{O}$ are the very broad (\sim 2 kHz) meso-H signals (m), which are taken as evidence for six-coordination; in accordance with this, these low-field meso-H signals are absent in *Aplysia* metMb.¹⁴ Note that such broad low-field resonances are observed in all E11 SW metMb mutants (Figure 2) but are absent in the E7 mutants (Figure 3).

The only narrow upfield shifted, resolved heme resonances are the vinyl H $_b$ s (q) observed in both SW metMbH $_2\text{O}$ and *Aplysia* metMb. All other resolved resonances in both proteins must come from noncoordinated distal amino acid side chain protons which experience dipolar shifts due to the large zero-field splitting for the high-spin ferric state.²⁵ For wild type (WT) SW metMbH $_2\text{O}$ (Figures 2A, 3A) we observe, in addition to the previously reported¹³ narrow methyl proton signals at \sim -4 and -5 ppm, a broad (\sim 2 kHz) and very rapidly relaxing signal with an area of about three protons at \sim -14 ppm which must originate from a methyl.

(30) Unger, S. W.; Lecomte, J. T. J.; La Mar, G. N. *J. Magn. Reson.* 1985, 64, 521-526.

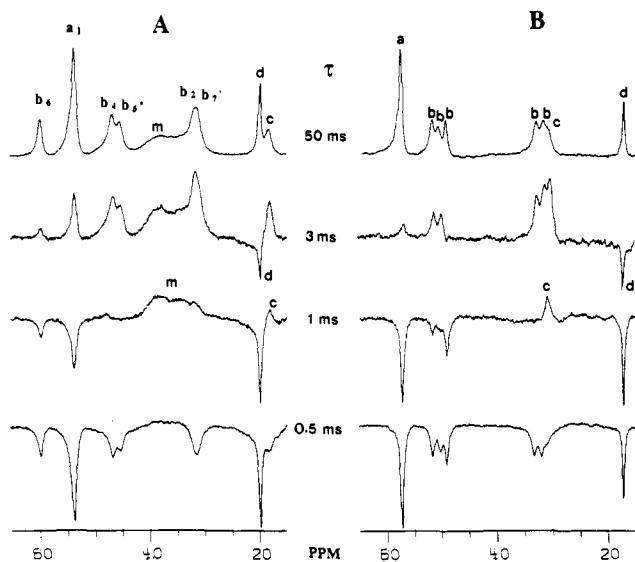


Figure 4. Partially relaxed 360-MHz ^1H NMR spectra of the down-field region in $^2\text{H}_2\text{O}$ at 25°C of SW WT metMb and His[E7]Val metMb as a function of delay time, τ , in an inversion-recovery T_1 determination. (A) For the shortest delay time, $\tau = 0.5$ ms, all the peaks are inverted. (B) For the delay time $\tau = 1$ ms, in the case of WT metMb, the meso-H's (m) have already relaxed and appear as positive peaks (~ 40 ppm). Note the absence of similar broad peaks in His[E7]Val mutant. Also note the appearance of the His C_βH peak (c) as a positive peak in both the proteins while all other one-proton peaks are inverted. (C) For the delay time $\tau = 3$ ms all peaks have recovered but for the 7- C_βH propionate (d) in both SW WT and His[E7]Val mutant and (D) for the delay time $\tau = 50$ ms fully recovered spectrum.

Aplysia metMb also exhibits a broad, rapidly relaxed, methyl signal (z) in the upfield region as reported previously.¹⁴ In the five-coordinate *Aplysia* metMb, the broad meso-H (m) resonances have been shown also to resonate upfield on the basis of isotope labeling.¹⁴

Relaxation Properties. The nonselective spin-lattice relaxation times, T_1 's, were determined by the inversion-recovery method for SW metMbH₂O. The T_1 values were determined by the null method and are accurate to $\pm 20\%$, which is sufficient for the present purposes. As found earlier at 500 MHz,³⁰ the four methyls (a) exhibit T_1 's ~ 4 ms, the vinyl and the propionate C_αH protons (b) yield T_1 's ≥ 2 to 5 ms, the His F8 C_βH (c), $T_1 \sim 1$ ms, the meso-H (m), $T_1 < 1$ ms, and the narrow 7-propionate C_βH (d) $T_1 \sim 8$ ms. The shorter T_1 for the His F8 C_βH (c) than that for propionate and vinyl C_αH s (b) has also been observed in high-spin resting state horseradish peroxidase.³¹ The T_1 's of *Aplysia* metMb exhibit very similar values,³² including a T_1 of ≤ 1 ms for the strongly upfield shifted methyl peak (z). The T_1 's for all the E7 mutants and Val[E11]Phe mutant were determined and T_1 's for the various resonances were essentially identical with that of SW metMbH₂O and *Aplysia* metMb (given in the supplementary material).

Resonance Assignments. (a) Low-Field Resonances. The four heme methyls, labeled a, for all the proteins studied are trivially identified by area. The SW Mb E11 mutants exhibit methyl line widths ~ 370 Hz comparable to that of the WT protein, while the E7 mutants display narrower lines, ~ 300 Hz. The nonselective T_1 's for all metMb mutant heme methyl protons are unchanged from that of SW metMbH₂O, ~ 4 ms. The six heme H_α (b) signals can be collectively differentiated from the His C_βH peak (c) on the basis of the shorter T_1 (~ 1 ms) for the His C_βH peak, c, than the other H_α peaks (≥ 2 ms), as evident clearly in the partially relaxed ^1H NMR trace for SW metMbH₂O (Figure 4A), and represented by a typical example from the SW metMb mutants, His[E7]Val (Figure 4B). Thus the rapidly relaxing single

proton peak (c) is assigned to His C_βH in each of the SW Mb E7 and E11 mutants studied. A signal with similar relaxation properties has been attributed earlier to a His F8 C_βH in *Aplysia* metMb.¹⁴

Partial assignment of heme methyls and propionate H_α 's was pursued in only one case with 1D NOEs. Saturation of His-[E7]Val SW metMb mutant peak b_7 gave $\sim 6\%$ NOE to b_7 and $\sim 1\%$ NOE to methyl a_8 identifying a pair of propionates $\alpha\text{-CH}_2$ near a methyl (data not shown). The pattern of a large shift spread of the b_7 , b_7 pair together with the lowest field shift for a_8 argue for the assignments a_8 , b_7 , b_7 to 8- CH_3 and 7- $\alpha\text{-CH}_2$ protons, respectively. It is likely that the heme methyl pattern is the same in all the mutants. The relatively narrow (~ 150 Hz) low-field peaks (d) observed near 20 ppm for all SW metMb mutants exhibits a longer $T_1 \sim 8$ ms and is assigned to the 7-propionate C_βH by analogy to a similar peak observed in SW metMbH₂O.

The only other detected low-field signal is the broad composite peak (m), ~ 40 ppm, shown to arise from meso-H's in SW metMbH₂O.¹³ This peak is observed with similar chemical shifts in all three E11 metMb mutants studied (Figure 2). For these mutants, the pattern of the low-field methyl and single proton resonances is remarkably similar to that of WT metMbH₂O. In contrast, all E7 mutants (Figure 3) fail to exhibit the broad, fast relaxing signals in the low-field window, even under extremely rapid pulsing conditions (not shown) which emphasize solely the meso-H signals. While the four methyl protons exhibit hyperfine shifts that are essentially invariant among the four E7 mutants studied (although different from WT), the single proton peaks exhibit remarkable variations in shifts among the E7 mutants (Figure 3).

(b) High-Field Resolved Resonances. The narrow peak (q) near ~ 7 ppm has been shown to arise from heme 2 and 4 vinyl H_β 's in SW (splits at 55°C), *Aplysia*, and model compounds. Such a peak(s), q, is detected in all of the mutant proteins. For the E7 mutants, we find upfield not only a broad resonance, consistent with intensity for three protons that must originate from the same group as peak z in SW metMbH₂O, but also either an additional peak (His[E7]Phe; Figure 3C) or a composite with intensity corresponding to more than three proton intensity (His[E7]Val; Figure 3D). Reconstitution of His[E7]Phe and His[E7]Val mutants with heme $>90\%$ perdeuterated at the meso positions yields holoprotein signals in which some of the upfield signal is lost or a portion of the intensity of the composite is clearly diminished corresponding to intensity of about two meso-H's; the other two meso-H's are likely under the upfield side of the diamagnetic envelope. Similar isotope labeling studies in *Aplysia* metMb have shown three upfield resolved meso-H signals ~ -15 to -35 ppm.¹⁴

The low-field region of the ^1H NMR spectra of the E11 metMb mutants is essentially unchanged from that of WT metMbH₂O (Figure 2); however the upfield region exhibits important changes. The broad (~ 1.5 kHz) fast-relaxing ($T_1 \sim 1$ ms) methyl peak z of SW metMbH₂O (Figure 3A) is absent in all of the E11 mutants, with a more weakly shifted, narrower peak appearing in the Val[E11]Phe and Val[E11]Ile mutants. The selective perturbation of the resonance z upon mutation at the E11 position dictates that the peak z must originate from one of the Val E11 methyls.

The assignment of peak z to a specific Val E11 methyl in SW metMbH₂O can be made on the basis of its short $T_1 \sim 1$ ms (Table I). Relaxation of heme methyl and noncoordinated amino acid side chain protons is dominated by proton-electron dipolar coupling, such that the relative relaxation rates are related to the inverse sixth power of the distance from the metal R, i.e.

$$T_{1i}/T_{1j} = R_{\text{Fe}-i}^6/R_{\text{Fe}-j}^6 \quad (1)$$

The methyls of Val E11 are 4.7 and 5.9 Å from the iron in the crystal structure, and the heme methyl is 6.1 Å from the iron. When a T_1 of 4 ms for the heme methyl is used, eq 1 predicts T_1 's of 0.8 ms for $\text{C}_{\gamma 2}\text{H}_3$ ($R_{\text{Fe}} = 4.7$ Å) and 4 ms for $\text{C}_{\gamma 1}\text{H}_3$ ($R_{\text{Fe}} = 5.9$ Å); the observed $T_1 \leq 1$ ms for the methyl signal z therefore dictates that it be assigned to $\text{C}_{\gamma 2}\text{H}_3$ of Val E11. There is no other

(31) Thanabal, V.; La Mar, G. N.; de Ropp, J. S. *Biochemistry* **1988**, *27*, 5400-5407.

(32) Pande, U.; La Mar, G. N. Unpublished results.

Table I. Separation of Hyperfine Shifts into Contact and Dipolar Contributions for Various metMbs

peak	assign	R^a	θ^a	G.F. ^b	δ_{obs}^c	δ_{dia}^d	δ_{hf}^e	δ_{dip}^f	δ_{con}^g	D^h
SW metMbH ₂ O										
z	E11 Val C ₇₂ H ₃	4.7	27	13	-14.1	-2.3	-11.8	-11.8	0.0	6.9
a	heme methyl	6.1	90	-4.4	76	3	73	4	69	
m	heme meso	4.5	90	-11	~37	10	~27	10	17	
c	His F8 C ₈ H	6.3	9	7.6 ⁱ	18.1	1.7	16.4	-6.9	23.3	
His[E7]Val SW metMb										
z	E11 Val C ₇₂ H ₃	4.7	27	13	-27	-2.3	-24.7	-24.7	0.0	13.8
a	heme methyl	6.1	90	-4.4	80.2	3	77	11	66	
m	heme meso	4.5	90	-11	-27	10	-37	26.8	-64	
c	His F8 C ₈ H	6.3	9	7.6 ⁱ	31	1.7	29.3	-18.6	47.9	
Aplysia metMb										
z	E11 Ile C ₈ H ₃	5.2	18	12	-27.2	-2.3 ^j	-24.9	-24.9	0.0	15.8
a	heme methyl	6.1	90	-4.4	80.5	3 ^j	77.5	9.2	68.3	
m	heme meso	4.5	90	-11	~-30	10 ^j	-40	23	-63	
c	His F8C ₈ H	5.9	27	7 ⁱ	23	1.7 ^j	21.3	-12.4	33.7	

^aDistances (Å) and angles (deg) obtained from the crystal structure of SW and *Aplysia*, respectively. ^bG.F. (geometric factor) = $(3 \cos^2 \theta - 1)r^{-3} \times 10^{26} \text{ cm}^2$. ^c δ_{obs} = experimentally observed chemical shift at 25 °C in ppm from DSS. ^d δ_{dia} = shifts from the NbCO complex obtained from ref 33. ^e $\delta_{\text{hf}} = \delta_{\text{obs}} - \delta_{\text{dia}}$. ^f $\delta_{\text{dip}} = \delta_{\text{dip}}$ is calculated by using eq 4 and the value of D is taken as 6.9 cm⁻¹, which was calculated from the dipolar chemical shifts of the distal Val and Ile using eq 4. ^g $\delta_{\text{con}} = \delta_{\text{hf}} - \delta_{\text{dip}}$. ^h D = value of D calculated by using eq 4 and substituting the observed dipolar chemical shift of the methyl group of distal Val and Ile, respectively. ⁱGeometric factors (G.F.) for both the C₈H's are similar and hence only one of the protons is considered. ^j δ_{dia} of these protons are taken to be same as those in SW metMb.

methyl group beside Val E11 C₇₂H₃ in Mb that can approach the iron close enough to experience the relaxation exhibited by peak z.

The assignment of the distal E11 residue, moreover, can be extended to *Aplysia* metMb, where a similar upfield three-proton signal z¹⁴ with $T_1 \sim 1$ ms must originate from one of the Ile E11 methyls. The use of eq 1 and the observed heme methyl $T_1 \sim 4$ ms predicts T_1 's of 1.5 and 5 ms for C₈H₃ ($R_{\text{Fe}} = 5.2$ Å)⁸ and C₇H₃ ($R_{\text{Fe}} = 6.3$ Å) of E11 Ile. Again, there are no other methyl groups close enough to the iron such that peak z of *Aplysia* metMb can be assigned to C₈H₃ of Ile E11. We therefore conclude that peak z in His[E7]Val is similarly from a methyl of E11 Val on the basis of its short T_1 (~1 ms).

Discussion

Hyperfine Shift Analysis. The observed shift, δ_{obs} , of a hyperfine-shifted proton is given by

$$\delta_{\text{obs}} = \delta_{\text{dia}} + \delta_{\text{hf}} \quad (2)$$

where the hyperfine shift, δ_{hf} , can have dipolar, δ_{dip} , and contact, δ_{con} , contributions

$$\delta_{\text{hf}} = \delta_{\text{dip}} + \delta_{\text{con}} \quad (3)$$

and δ_{dia} is the shift in an isostructural diamagnetic complex taken as MbCO in our case.³³ The essentially axial dipolar shift (δ_{dip}) results from the substantial zero-field splitting, D , characteristic of the ⁶A state of ferric heme proteins^{25,34} and is given by

$$\delta_{\text{dip}} = \frac{-28g^2\beta^2}{k^2T^2} \frac{(3 \cos^2 \theta - 1)}{R^3} D \quad (4)$$

where θ is the angle between the iron-proton vector R and the heme normal. R and θ are obtained from the crystal coordinates (Table I). For a noncoordinated amino acid, δ_{con} is essentially zero, and,

$$\delta_{\text{dip}} = \delta_{\text{obs}} - \delta_{\text{dia}} \quad (5)$$

For SW metMbH₂O, the noncoordinated amino acid which has methyls in the immediate vicinity of the iron is E11 Val with one of the methyls, C₇₂H₃, close to the iron, and it is expected to have substantial dipolar shift. The other methyl, C₇₁H₃, is pointed away from the iron and experiences negligible dipolar shift (data not shown). The experimental δ_{dip} of Val E11 C₇₂H₃ is ~-12 ppm (Table I), and substituting into eq 4 yields $D = 6.9 \text{ cm}^{-1}$. This is in reasonable agreement with the D value of 9.5 cm⁻¹ reported

from IR studies³⁵ of SW metMbH₂O at 4 K. Hence, both the observed relaxation properties and dipolar shift indicate that peak z arises from Val E11 C₇₂H₃ in SW metMbH₂O.

For two nonequivalent protons in a complex, the relative dipolar shifts are given by the relationship

$$\delta_{\text{dip}}^i / \delta_{\text{dip}}^j = (3 \cos^2 \theta_i - 1)R_i^{-3} / (3 \cos^2 \theta_j - 1)R_j^{-3} \quad (6)$$

By using the above equation, the Val E11 C₇₂H₃ dipolar shifts, and the geometric factors given in Table I, δ_{dip} is calculated for the heme methyls, meso-H's, and F8 C₈H of SW metMbH₂O all of which also exhibit contact shifts (Table I). From the calculated δ_{dip} and the available δ_{dia} and δ_{obs} , δ_{con} can be calculated with eq 1. The results are shown in Table I.

Aplysia metMb has a distal Ile instead of Val. The crystal coordinates of *Aplysia* metMb⁹ show that the C₈H₃ has a geometric factor almost identical with that of E11 C₇₂H₃ of SW (Table I): the Ile C₈H₃ points away from the iron and hence experiences negligible dipolar shift. δ_{dip} is calculated as ~-25 ppm for C₈H₃ with eq 1. The much larger δ_{dip} (~-25 ppm) for C₈H₃ of E11 Ile in five-coordinate *Aplysia* metMb than for Val E11 C₇₂H₃ in six-coordinate SW metMbH₂O, in spite of very similar geometric factors for the two methyls, dictates that *Aplysia* metMb must have a substantially larger zero-field splitting, D . Equation 4 predicts ~16 cm⁻¹ for the latter protein which is twice as that of the former. The predicted δ_{dip} via eq 5 and the calculated δ_{con} via eq 3 for other resonances of *Aplysia* metMb are shown in Table I.

We note that the His[E7]Val metMb mutant differs from the WT in having not only upfield meso-H shifts as in *Aplysia* metMb but also low-field shifted heme methyls and a much more upfield shifted Val E11 C₇₂H₃ (z). Hence we conclude that this mutant is five-coordinate like *Aplysia* metMb. Assuming that the orientation of Val E11 is unaltered in this mutant,³⁶ the $\delta_{\text{dip}} \sim -24$ ppm indicates that D is comparable to that of *Aplysia* metMb and twice that of WT SW metMbH₂O (Table I).

Detailed studies of a number of high-spin ferric complexes, including hemes, have already shown that they not only exhibit positive D values but also the magnitude of D increases significantly when the axial ligand field is weakened.²⁵ Between SW metMbH₂O and *Aplysia* metMb, the effective axial ligand field would be highly reduced in the five-coordinate *Aplysia* metMb in complete agreement with the observation of a much larger positive D value in *Aplysia*. Hence the loss of water at the sixth

(35) Brackett, G. C.; Richards, D. L.; Caughey, W. S. *J. Chem. Phys.* 1971, 54, 4383-4401.

(36) C₇₂H₃ chemical shifts are essentially unaltered in the diamagnetic MbCO complex (difference in chemical shift is ~0.1 ppm) (Chiu, M.; Sligar, S. G., unpublished results).

(33) Dalvit, C.; Wright, P. E. *J. Mol. Biol.* 1987, 194, 313-327.

(34) Kurland, R. J.; McGarvey, B. R. *J. Magn. Reson.* 1970, 2, 286-301.

position in a ferric high-spin hemoprotein should manifest itself in larger zero-field splitting and therefore larger dipolar shifts. Moreover the ~ 12 ppm δ_{dip} for Val E11 C_βH_3 in SW metMbH₂O and the ~ 25 ppm δ_{dip} for Ile E11 C_βH_3 in *Aplysia* metMb indicate that the heme methyls experience 5 and 10 ppm downfield dipolar shifts, respectively (Table I). Therefore, the difference in D values and the consequent δ_{dip} completely account for the mean 5-ppm low-field bias of the four methyls in *Aplysia* metMb relative to that of SW metMbH₂O. The same ~ 5 -ppm low-field bias relative to SW metMbH₂O for the heme mean methyl shifts is observed in SW mutant metMb His[E7]Val, confirming that the His \rightarrow Val substitution leads to loss of the coordinated H₂O.

The His F8 C_βH hyperfine shift experiences both low-field contact and upfield dipolar shifts (see Table I). Since the contact shift depends critically on orientation of the C_βH relative to the imidazole plane, quantitative comparison of His C_βH shifts between SW and *Aplysia* metMb is not useful. However, among the SW mutants the His F8 orientation is unaltered, indicated by the largely invariant heme contact shift pattern in the low-spin cyano met complexes. Since the upfield δ_{dip} is much larger in His[E7]Val than that in WT, the larger low-field δ_{obs} dictate an even larger His C_βH δ_{con} for the His[E7]Val mutant than WT (Table I). The covalency (and hence the degree of σ -spin delocalization) in a complex is modulated by the strength of its trans ligand, the "trans effect", where weakening the ligand field strength of a ligand trans to the His F8 is expected to increase the His-Fe covalency, and hence the contact shift. The absence of a coordinated H₂O is clearly a decrease in ligand field, and hence the His F8 C_βH in a five-coordinate protein should exhibit significantly larger contact shift than in a six-coordinate protein. We note that all the E7 mutants, and in particular His[E7]Val, exhibit larger low-field His F8 C_βH contact shifts than SW metMbH₂O.

NMR Probes for Water Coordination. The difference in D between five- and six-coordinated metMbs accounts quantitatively for the difference in the mean heme methyl hyperfine shifts. In contrast, the predicted change (via eq 3) in δ_{dip} for meso-H upon loss of H₂O is a 10-ppm downfield bias. Instead, a 50–80 ppm upfield bias is observed in proteins (Table I) as well as in model compounds. Hence, as concluded previously, the meso-H shift changes are dominated by contact shift changes that are not understood. Nevertheless, we note that the characteristic change in low-field to upfield meso-H contact shifts upon loss of the sixth ligand is accompanied by the more quantitatively understood magnetic and electronic properties, such as larger D values. This corresponds to predictable ratios of upfield E11 and downfield heme methyl dipolar shift changes and increased axial His-Fe contact shifts. These latter observations, therefore, provide important confirmation of the NMR probes for differentiating between five- and six-coordinated ferric proteins, and an effective comparison should utilize all of them, particularly among a series of mutants.

Comparison of Mutants. It is observed that the low-field region of ¹H NMR spectra of the E11 mutants (Figure 2) is essentially invariant and identical with that of the WT metMbH₂O. In particular, the meso-H shifts are low-field, and both the mean heme methyl and His F8 C_βH shifts are unaltered (Table II). Hence, substitution of the E11 Val residue with other nonpolar amino acids retains the coordinated H₂O. In contrast, substituting the E7 His with Val clearly leads to a five-coordinated heme by all ¹H NMR criteria, low-field bias of heme methyls and His C_βH , upfield bias of E11 Val, and direction change of the chemical shift from low-field to upfield for meso-H. Analysis of the ¹H NMR spectra for the remaining E7 mutants and the tabulated mean heme methyl, meso-H, and F8 C_βH chemical shifts reveal that all the mutants fall into two distinct classes. For the His[E7]Val and His[E7]Phe mutants, the meso-H's are clearly resolved upfield, and hence both must be solely five-coordinate. For the His[E7]Gly and His[E7]Gln mutants, while the heme methyls are low-field shifted by ~ 5 ppm, the His C_βH s are downfield shifted to a lesser extent than in His[E7]Val. In addition, the meso-H shifts, while not downfield, do not appear to be resolved

Table II. Comparison of Solvent Isotope Effects on Heme Methyl Shifts in SW metMb Mutants^a

metMb	meso-H in ² H ₂ O	F8C _β H in ² H ₂ O	mean heme methyl shifts		% change ^b
			in ² H ₂ O	in H ₂ O	
wild type	~ 40.0	18.1	76.1	74.9	1.6
His[E7]Phe	-30.5	32.3	80.5	80.5	0
His[E7]Val	~ -27	~ 31	80.2	80.3	0
His[E7]Gly	<i>c</i>	23.5	80.0	79.8	0.3
His[E7]Gln	<i>c</i>	23.9	80.0	79.8	0.3
Val[E11]Ala	~ 40	~ 19	75.0	74.5	0.7
Val[E11]Phe	~ 37	~ 19	75.5	74.5	1.3
Val[E11]Ile	~ 37	19.5	75.2	74.1	1.3

^a Observed chemical shifts in ppm from DDS at 25 °C; uncertainty in chemical shift ± 0.05 ppm. ^b Percent change in chemical shift, $[(^2\text{H}_2\text{O} \text{ shift} - ^1\text{H}_2\text{O} \text{ shift}) / ^1\text{H}_2\text{O} \text{ shift}] \times 100$. ^c Not observed.

in the upfield window, in that the peak z does not have the intensity to cover more than one meso-H. Moreover, even peak z, which must arise from the Val E11 $\text{C}_\gamma\text{H}_3$, experiences upfield dipolar shifts intermediate between those of six-coordinate WT and five-coordinate His[E7]Val metMb. These observations for the His[E7]Gly and His[E7]Gln mutants suggest an environment intermediate between five- and six-coordinate, but much closer to the former. Since only one set of resonances is observed, these results indicate a partial occupancy of H₂O at the sixth position, with the five- and six-coordinate systems interconverting rapidly.

Resonance Raman (RR) studies¹⁹ have been performed in His[E7]Phe, His[E7]Val, His[E7]Gly, and Val[E11]Ala and other E7 and E11 mutants. Our NMR results are in agreement with the RR studies of the E7 mutants except for His[E7]Gly mutant: RR studies suggest that the His[E7]Gly mutant is 6-coordinate whereas NMR data argue for only fractional H₂O coordination. A preliminary X-ray structure study of the His[E7]Gly mutant is consistent with a fractional H₂O occupation at the heme.³⁷

Isotope Effects on NMR Spectral Parameters. We have shown previously that changes in solvent isotope composition lead to a large isotope effect on methyl contact shifts in six-coordinates SW metMbH₂O and none in five-coordinate *Aplysia* metMb.²⁴ The isotope effects were interpreted in terms of variable H bonding between the E7 His and the axial H₂O. The ²H₂O/¹H₂O difference in shifts (Table II) reveals a 0.8–1.5 ppm low-field bias in ²H₂O relative to ¹H₂O for all the E11 mutants, consistent with E7 His interaction with a bound water. The isotope effect in the His[E7]Val and His[E7]Phe mutants is negligible, as found previously for five-coordinate *Aplysia* metMb. However, both His[E7]Gly and His[E7]Gln mutants exhibit a clear, albeit weak isotope effect of 0.3 ppm, which is intermediate between that of known six-coordinated and five-coordinated metMbs. This small isotope effect supports fractional water occupation in the His[E7]Gly and His[E7]Gln mutants. Furthermore, the correlation between shift trends and isotope sensitivity confirms the utility of the isotope effect as an additional probe for axial water coordination.

Structural Perturbations Due to H₂O Binding. It was noted above that the low-field chemical shifts are essentially invariant among all E11 mutants (Figure 2). However for the E7 mutants, while the four heme methyl chemical shifts are invariant, the single proton chemical shifts display systematic variation (Figure 3). Such variations in single proton resonances, despite unaltered spin density as reflected by the invariant methyl chemical shifts, must reflect change in orientation of side chain(s). The NOE assignment in the His[E7]Val metMb mutant confirms that the 7-propionate C_αH has moved and rotated relative to its position in the WT. Moreover, the 7-C_αH probably is the furthest low-field shifted single proton peak in all the metMb mutants. Hence 7-C_αH resonances appear low-field in the following order: Phe > Val > Gly \sim Gln > WT. The conversion of a six-coordinate to five-coordinate heme is expected to cause the Fe to move out of the heme plane and a concomitant doming of the heme. In

(37) Phillips, G. N. Personal communication.

Table III. Comparison of the Heme Methyl and Meso Chemical Shifts of metMb in Natural Genetic Variants^a

	mean methyl shift	meso-H shift
<i>Aplysia</i> (25 °C, pH 6.0) ^b	80.5	~-30
shark (25 °C, pH 6.0) ^c	79.8	~-20
CNBr modified SW Mb (23 °C, pH 7.0) ^d	80.3	~-35 ^e
<i>Glycera</i> (major) (22 °C, pH 6.8) ^f	79.8	<i>j</i>
(minor)	80.2	
elephant (25 °C, pH 6.5) ^g	81.3	<i>j</i>
sperm whale (25 °C, pH 6.6) ^h	76.0	~40
equine (25 °C, pH 6.0) ⁱ	75.8	<i>j</i>
yellow fin tuna (25 °C, pH 6.0) ^j	74.6	<i>j</i>

^aChemical shifts in ppm from DSS measured in D₂O. ^bFrom ref 14. ^cFrom ref 15. ^dFrom ref 38. ^eMeso chemical shifts were assigned by ²H NMR from ref 39. ^fFrom ref 15. The minor isomer is rotated 180° about the α - γ meso axis. Note that the orientation of the heme in the minor form of *Glycera* is the major form in SW metMbH₂O. ^gFrom ref 17. Chemical shifts of the major of the two interconverting forms in solution. ^hFrom ref 13. ⁱUnpublished results. ^jNot reported.

SW metMbH₂O, the 7-propionate group forms a salt bridge with His FG3 N₃H on the proximal side, and any doming of the heme probably requires some accommodation of this propionate orientation. Since the trend in 7-C _{α} H shifts is the same as that observed for the position of the six-coordinate–five-coordinate equilibrium, we propose that the 7-C _{α} H chemical shifts may serve as a probe for doming of the heme. X-ray studies of the mutants should reveal the nature of the change in the orientation in the mutants and provide a calibration for the observed chemical shift changes.

Water Coordination in Natural Genetic Variants. The ¹H NMR data reported for a variety of high-spin ferric Mbs and monomeric Hbs are shown in Table III.^{13–17,38} Only the collective four heme methyls have been identified with certainty in all systems, and the meso-H chemical shifts have been assigned by isotope labeling in the case of *Aplysia*,¹⁴ shark metMb,¹⁵ and CNBr reacted SW metMb.³⁹ It is clear that the mean heme methyl shift for all the proteins clusters near either SW metMbH₂O (~76 ppm) or five-coordinated *Aplysia* metMb (~80 ppm). Thus the mean methyl shift argues for five-coordinate in shark (E7 Gln), CNBr reacted SW metMb, and *Glycera* (E7 Leu) metHb. Upfield signals arising from meso-H's, where reported, are in agreement with the observations made for heme methyl chemical shifts.

Previous ¹H NMR studies of elephant (E7 Gln) metMb¹⁷ had identified an isotope-dependent equilibrium between two protein forms which interconvert slowly on the NMR time scale. Originally, this multiplicity of solution isomers was attributed to alternate H-bonding configurations between the E7 Gln side chain and the bound H₂O. However, one (the major) of the two isomers exhibits heme methyl shifts with a mean shift of 81 ppm (Table II), suggesting that the two isomers differ in only one having H₂O bound, and that the major isomer in solution is, in fact, five-co-

ordinate. The present observation of a dominant five-coordinate elephant metMb at acidic pH is consistent with the earlier kinetic studies of NO binding, which showed ~10³ faster ligation rates in elephant than that in SW metMbH₂O.¹¹ The conclusion that *Glycera* metHb is five-coordinate is also consistent with the observation of faster NO binding rates.¹²

We note that the conclusions on H₂O coordination for point mutants parallel those reached for similar natural genetic variants. Thus, His[E7]Val mutant and *Aplysia* (E7 Val) (as well as *Glycera* Hb, E7 Leu) are five-coordinate. E7 Gln leads to strong destabilization of bound H₂O and hence only fractional occupation in elephant metMb as well as in the E7 Gln point mutant, though Gln is capable of H bonding to the bound H₂O. The parallel between the synthetic point mutants of SW Mb and the natural genetic variants with respect to H₂O coordination in the met form, in spite of very little overall sequence homology, suggests that the nature of the E7 residue is the controlling factor in stabilizing the bound H₂O.

Distal Features for H₂O Binding. The properties of the distal residue can be described on the basis of H-bonding capabilities, steric bulkiness, and/or hydrophobicity (polarity). It is clear that among the E7 residues considered, His is unique in strongly stabilizing a bound H₂O and this is due to H bonding⁴⁰ (depicted in Figure 1). However, retaining the potential E7 H-bonding interaction with bound H₂O, as in the case of the His[E7]Gln mutant or elephant metMb, results in only fractional H₂O coordination. The Gln side chain, though of similar length and volume as the imidazole of His, has greater flexibility, and entropic factors could destabilize the binding of H₂O to the heme. The complete loss of axial water in the His[E7]Val and His[E7]Phe metMb mutants indicates that the stability of bound H₂O is significantly reduced when the potential H bonding of the E7 residue is abolished. Among the hydrophobic E7 side chains, complete loss of coordinated water occurs for both the bulky Phe and the smaller Val. However, as the size of the E7 side chain is further reduced to Gly, weak fractional water coordination is reintroduced. The fractional H₂O binding in Gly but not Val could be due to the larger pocket generated for the smaller Gly side chain and/or because of the increased polarity of Gly as against Val.⁴¹ It is clear that a combination of H bonding and steric and hydrophobic interactions control the binding of H₂O to the iron(III) in Mbs and that further studies with other E7 mutants are necessary to sort out these individual contributions.

Acknowledgment. This work was supported by grants from the National Institute of Health, HL-16087 (G.N.L), HL-22252 (K.M.S), and GM-33775 (S.G.S).

Supplementary Material Available: Tables of one-proton chemical shifts and the solvent isotope effect on the heme methyl chemical shifts of all the E7 and E11 mutants (1 page). Ordering information is given on any current masthead page.

(38) Shiro, Y.; Morishima, I. *Biochemistry* **1984**, *23*, 4879–4884.

(39) Morishima, I.; Shiro, Y.; Wakino, T. *J. Am. Chem. Soc.* **1985**, *107*, 1063–1065.

(40) Caughey, W. S. In *Hemes and Hemoproteins*; (Eds. Chance, B., Estabrook, R. W., Yonetani, T., Eds.; Academic Press: New York, 1966; pp 43–48.

(41) Chothia, C. *Annu. Rev. Biochem.* **1984**, *53*, 537–572.